ELSEVIER

Journal of Fluids and Structures 25 (2009) 794–814

JOURNAL OF FLUIDS AND STRUCTURES

www.elsevier.com/locate/jfs

Impact interaction of cylindrical body with a surface of cavity during supercavitation motion in compressible fluid

V.D. Kubenko*, O.V. Gavrilenko

National Academy of Sciences, S.P. Timoshenko Institute of Mechanics, 3, Nesterov Str., Kyiv 03057, Ukraine

Received 21 December 2007; accepted 12 October 2008
Available online 8 July 2009

Abstract

The paper deals with the early stage of impact of a solid cylindrical body on the surface of a cylindrical cavity for zero and non-zero gap between the cavity surface and the body surface. As a result, the stated mixed non-stationary boundary value problem with the unknown variable in the time boundary is formulated. Its solution is reduced to a joint solution of an infinite system of linear integral Volterra equations of the second kind and the differential equation of the body movement. In the case of simplified formulation, the solution is reduced to the infinite sequence of the linear integral Volterra equations. Hydrodynamic and kinematic characteristics are also obtained.
© 2009 Elsevier Ltd. All rights reserved.

Keywords: Compressible fluid; Cylindrical body; Cylindrical cavity; Non-stationary interaction; The varying field of contact; Finite and zero gap; Supercavitation

1. Introduction

The construction of underwater vehicles using the principles of so-called supercavitational motion is one direction of sea transport development. The phenomenon of supercavitation allows one to reduce considerably the hydrodynamic resistance of a liquid. It occurs when a cavity is formed from water vapour or gas bubbles upstream of a body submerged in a fast-moving stream. If the moving object is completely surrounded by a renewable gas shell, resistance to body movement is considerably reduced. The body, in fact, moves in a gas-vapour cavity, having contact with the liquid only in its frontal part, which is equipped with a cavitator. The principles of hydrodynamics of high velocities have been developed and formulated in a monograph by Logvinovich (1969). Over the last decade, research on supercavitational motion has been carried out in Russia, USA and Ukraine. Rates of movement, close to sonic velocity in water, have been obtained in the laboratory environment (Savchenko et al., 1998). The perspectives of application are quite attractive, and it elicits interest among researchers for the problem of supercavitation as a problem of hydromechanics concerning high-speed movement. Many modern results in this direction can be seen in papers of Lu, He and Wu (2000) and Young (2007).

One of the peculiarities of the process mentioned above is the almost inevitable lateral motion of the body in the cavity due to instability of the primary (longitudinal) movement. Such a lateral motion develops in a wide range of velocities and consists of alternate impacts of the body with the lower and upper parts of the cavity surface. This undesirable phenomenon leads to the loss of energy in the primary movement and can cause its cessation. Study of

*Corresponding author. Tel.: +380 44 456 12 80; fax: +380 44 456 03 19.
E-mail address: vdk@inmech.kiev.ua (V.D. Kubenko).

0889-9746/$ - see front matter © 2009 Elsevier Ltd. All rights reserved.
doi:10.1016/j.jfluidstructs.2008.07.007

Nomenclature

C	sound velocity
d	the gap between the body surface and the cavity surface
$J_1(x)$	Bessel cylindrical function
F	hydrodynamic force
$K_n(sr)$	McDonald cylindrical functions of imaginary argument
p	hydrodynamic pressure
R_b	certain linear dimension (cylinder radius)
R_c	cavity radius
r, θ	polar coordinates
t	time
V	velocity of cavity surface deformation
$v_0(t)$	velocity of the body penetration into fluid
x, z	Cartesian coordinates
z^*	depth of penetration
μ	linear mass of the body
ρ	fluid density
φ	wave potential

lateral impact motion and the establishment of regularity of its existence and development should be very useful, since it can lead to means of stabilization the longitudinal movement. Research on this matter was conducted mainly on the assumption of incompressible liquid (Savchenko et al., 1999; Parushev, 2002). The model of incompressible liquid does not provide reliable results on the early stage of impact interaction (according to this model, the value of the hydrodynamic pressure at the initial moment of interaction attains an infinitely large value, which is contrary to common sense). Additionally, research on this process seems to be expedient for an arbitrary ratio of specific cross-section values of the cavity and the body. It can be supposed that, for near cross-sections of the body and the cavity, stabilization of the basic (longitudinal) motion is rather relevant, at least in terms of energy.

Kubenko (2006) suggests the foundations of a relevant approach to the research of impact interaction of a rigid long circular cylindrical body with the surface of a circular cylindrical cavity in an ideal compressible fluid. In the general case, a non-stationary mixed boundary value problem of hydromechanics with an unknown variable boundary is formulated. The asymptotic solution is obtained for the initial stages of the interaction. For the case when the radius of the body cross-section is substantially smaller than the cavity radius, a numerical solution is obtained.

The present paper, an extension of the paper by Kubenko (2006), suggests a technique and derives a numerical solution for an arbitrary ratio of radii of cavity and body cross-sections. The analysis of peculiarities of the impact interaction process, depending on initial physical and mechanical parameters, is performed. The comparison of numerical and asymptotic solutions is carried out.

In Section 2, a statement of the nonstationary initial boundary value problem with the unknown time-dependent boundary is given. The stated problem consists of the combined system of equations: the hydrodynamic part (which describes a process of interaction between the body and the fluid); the equation of body motion across the cavity surface; and the relation for determination of boundary points of the varying contact domain. Corresponding boundary conditions are given separately on the body-fluid contact surface and on the free surface of the cavity. In general, this nonlinear problem requires corresponding methods of solution, which are developed for two specific cases of a ratio of the cross-section specific dimensions of the body and the cavity: (i) for small finite difference in radii and (ii) for coincidence of the radii, in Sections 3 and 4, respectively.

We shall expand the unknown quantities into Fourier series. To solve the auxiliary non-mixed problem, we will use the Laplace transform in time. In all cases, concerning the coefficients of corresponding Fourier series for pressure (velocity), a resolving infinite system of Volterra integral equations of the second kind is obtained. Such a system should be solved jointly with the equation of body motion and the relation determining the contact area. The conventional integral equations are also presented; it allows one to obtain the approximate solution of the problem with much less effort. In Section 5 the asymptotic solution of the problem for all three cases corresponding to the initial stage of the interaction is obtained. In Section 6 the numerical solution for Cases 1 and 2 is proposed as the one most often used in practice. Finally, in Section 7 the analysis of results obtained is carried out.

It should be mentioned that the present study considers the fluid at rest. Solution of the problem on the body cross-impact motion in a cavity, taking into consideration axial movement of fluid as well as the evaluation of the contribution to the process made by the impact on water and the mentioned motion, will be carried out separately.

2. Problem statement

As previously mentioned in the Introduction, it is an experimentally established fact (Savchenko et al., 1998) that under high velocity of motion a cavity develops around the body. A characteristic of the generating ellipsoid-shaped

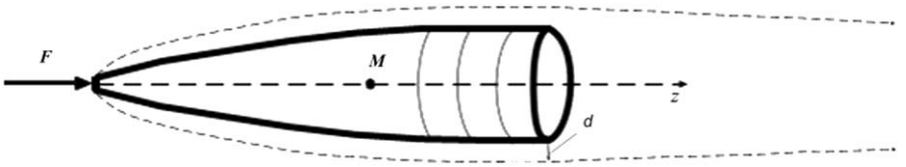

Fig. 1. Body moving in cavity.

supercavity is its big comparative elongation—aspect ratio of 70 to 200. The moving body is fully inside the cavity, having contact with it only in its front part.

Hence, the drag is applied to the body front-section, i.e., ahead of its centre of mass that causes violation of the classical condition of motion stability in a continuum—Fig. 1. Because of that, with velocity of the body movement in a water around 300–1000 m/s, the existence of initial perturbations in the angle of attack and angular velocity of the movement leads to lateral motion of a body and impact interaction of its rear end with interior wall of the cavity (Savchenko, 1998; Savchenko et al., 1999). In this case, the body may undergo steady or decaying periodic lateral motions accompanied by alternating impacts at the upper and lower walls of the cavity. To reduce losses of energy of the primary motion and to eliminate possible instability, one should know how to calculate the law of the transverse movement of the body within the supercavity. The present study is devoted to the generation of solution methods for this problem and to the production of numerical results illustrating various solution approaches.

Since the longitudinal dimensions of the body and the cavity essentially exceed their transverse dimensions (and the latter for the body and the cavity slightly differ from each other), it would be appropriate to perform the following mathematical modelling of the process of impact interaction of the body with the cavity in the supercavitation flow, which is valid for cross-sections far enough removed from the body ends.

An indefinitely long circular cylindrical cavity with radius R_c in an infinite fluid is considered. The cavity contains a body shaped as a rigid circular cylinder of radius R_b. The gap between the body surface and the cavity surface is denoted as d, where $d = R_c - R_b$. We shall consider the motion in a certain cross-section of the cavity and, therefore, we restrict ourselves by considering the plane problem. It is assumed that at a certain moment at time $t = 0$, the body reaches an interior surface of the cavity and starts penetrating through it with the initial velocity $v_0 = v_0(0)$. It is necessary to determine the hydrodynamic loading acting on the body and the law of body motion.

The body-fluid interaction stipulates, on the one hand, the appearance of acoustic waves, which carry away a portion of the impact energy and, on the other hand, the change of velocity of the body motion toward motion in the opposite direction.

The adequate simulation of such a process demands a solution of the coupled system of equations consisting of a hydrodynamic part, which describes motion of fluid under the impact penetration, and the equations of the body motion. The specified system should be supplemented with the appropriate boundary and initial conditions. Obviously, it is necessary to formulate various conditions on the surface of the body-fluid contact and on the free surface of the cavity. In the contact area, the condition of impermeability of the body surface (equality of normal to the surface velocities of the body and the fluid is naturals); on the free surface of the cavity, the pressure should be constant (for simplicity it is possible to accept it as zero).

It is necessary to notice that, during penetration of the body into the fluid, the position of boundary points on the cavity surface separating the area of contact from the action free area is not generally given; the mentioned points move along the surface with an unknown velocity and their position is determined at each time instant from the solution of the general coupled problem.

Initial conditions are also obvious; for the body, the initial position and the initial value of velocity $v_0 = v_0(0)$ are given. Here $v_0(t)$ is the required velocity of the body penetration into the fluid medium, while at the initial time instant, the fluid is at rest.

We assume that, in contrast to the longitudinal motion, the velocity of lateral motion of the body in the cavity v_0 is much less than the sound velocity in the fluid (nevertheless, for the purpose of considering a part of the impact energy carried away by acoustic waves, we shall not neglect compressibility of the fluid), with viscosity being negligibly small. In effect, one can consider the fluid as an ideal compressible one. It is natural to suppose, that the depth of body penetration through the initial cavity surface is small. It allows one to use a linear wave equation (a so-called acoustic approximation) for the description of fluid motion (Morse and Feshbach, 1958) and, in addition, to prescribe the boundary conditions on an undistorted surface of the cavity.

Thus, the above considerations allow one to formulate the initial mixed boundary value problem with the previously unknown space- and time-changing boundary.

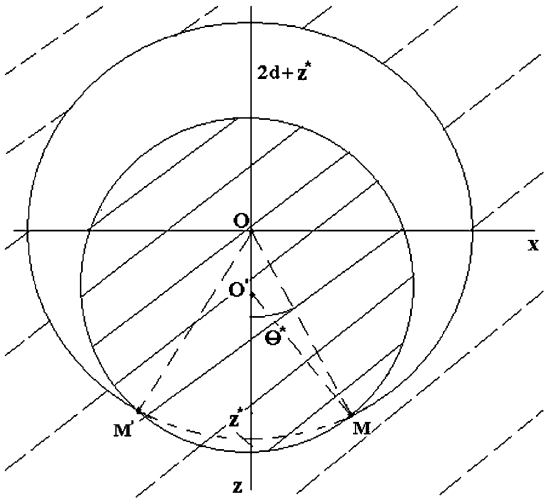

Fig. 2. Scheme of impact interaction of cylindrical body with the surface of cavity.

Let us initiate the mathematical formulation of the problem, the geometrical parameters of which are shown in Fig. 2. We shall introduce dimensionless variables for subsequent consideration:

$$\overline{x}=\frac{x}{R_c},\quad \overline{z}=\frac{z}{R_c},\quad \overline{r}=\frac{r}{R_c},\quad \overline{t}=\frac{Ct}{R_c},\quad \overline{p}=\frac{p}{\rho C^2},\quad \overline{V}=\frac{V}{C},\quad \overline{\mu}=\frac{\mu}{\pi\rho R_c^2},\quad \overline{F}=\frac{F}{\rho C^2 R_c}. \tag{2.1}$$

Here, x, z are Cartesian coordinates, r, θ are polar coordinates (the z-axis coincides with the direction of the body lateral motion) with a pole at the center of the cavity, t is time, p is hydrodynamic pressure, V is velocity of cavity surface deformation, C is sound velocity, ρ is fluid density, R_c is a certain linear dimension (the radius of the cavity), μ is the lineal mass of the body (according to Eq. (2.1), it is referred to a mass of the fluid displaced by the body per unit of length), and F is hydrodynamic force. Dimensionless notation (2.1) is used in what follows, therefore overbars are omitted.

The motion of the ideal compressible fluid is described by the wave potential, which satisfies the equation

$$\frac{\partial^2\varphi}{\partial r^2}+\frac{1}{r}\frac{\partial\varphi}{\partial r}+\frac{1}{r^2}\frac{\partial^2\varphi}{\partial\theta^2}-\frac{\partial^2\varphi}{\partial t^2}=0 \tag{2.2}$$

and the pressure and velocity of the fluid are defined by

$$p=-\frac{\partial\varphi}{\partial t},\quad V=\operatorname{grad}\varphi$$

Let us formulate the boundary conditions on the surface of the cavity $r=1$. As shown in Fig. 2, the points with the values of polar angle θ^* and $-\theta^*$ separate the contact area of the body with the cavity from the free surface of the cavity. Thus, the boundary condition in the contact area consisting of equality of normal velocities is the following:

$$\left.\frac{\partial\varphi}{\partial r}\right|_{r=1}=v_0(t)\cos\theta,\quad |\theta|<\theta^*. \tag{2.3}$$

The second condition, imposed on the desired solution in the contact area, suggests the impossibility of the appearance of areas with negative pressure

$$p|_{r=1}\geqslant 0,\quad |\theta|<\theta^*. \tag{2.4}$$

On the free part of the surface of the supercavity, a pressure

$$\left.\frac{\partial\varphi}{\partial t}\right|_{r=1}=0,\quad |\theta|>\theta^* \tag{2.5}$$

is given.

Expressions (2.3)–(2.5) consider the present symmetry with respect to z. It is also necessary to take into account the damping condition of wave disturbances at infinity

$$\varphi \to 0, \quad r \to \infty \tag{2.6}$$

The initial conditions for the potential of initially rest fluid are

$$\varphi|_{t=0} = \left.\frac{\partial \varphi}{\partial t}\right|_{t=0} = 0 \tag{2.7}$$

Finally, the equation of body motion is

$$\mu \frac{dv_0(t)}{dt} = -\frac{F(t)}{\pi}, \quad v_0(0) = v_0, \tag{2.8}$$

Here, $F(t)$ is hydrodynamical force of fluid resistance (the drag) to the lateral motion of the body, which can be calculated as:

$$F(t) = 2\int_0^{\theta^*} p(t,\theta)\cos\theta\, d\theta. \tag{2.9}$$

Let us recall that $p(t,\theta)$ is the fluid pressure in the contact area.

The angle θ^* is a polar angle of an intersection point of the circle—the boundary of the supercavity and the circle, which is the contour of the body; it is determined from a geometrical problem depending on the ratio of characteristic dimensions of the cavity, body as well the unknown depth of penetration $z^* = \int_0^t v_0(\tau)\, d\tau$ as follows:

$$\theta^* = \arccos\left(\frac{(z^*)^2 + 2d(z^*+1)}{2(d+z^*)}\right). \tag{2.10}$$

It must be noted that this relation does not take into account the so-called opposing motion of the liquid, which can vary the contact domain. But, during an early stage of the process of interaction, the contact domain varies rapidly (even with supersonic velocity at an initial time interval), and the liquid compressibility is a more important factor in comparison to the opposing motion (Logvinovich, 1969). Therefore, it can be expected that Eq. (2.10) is approximately true for determining the contact area.

It is necessary to note, that the dimensionless gap d is defined as $d = 1 - R_b/R_c$.

Relations (2.2)–(2.10) represent a mathematical formulation of the considered problem. In a general case, the problem is nonlinear due to imposed condition (2.4), and also because, specifically, the equation of motion (2.8) on its right-hand side contains complicated functional dependence on the penetration depth z^* (see Eq. (2.10)), which in turn is determined through the sought velocity of the body motion $v_0(t)$.

The character of lateral movement of the body in the cavity, as well as the overall movement, essentially depends on the dimension of the gap between the surface of the body and the cavity (Putilin, 2000). Generation of the motion with minimal gap can require less consumption of energy. On the other hand, minimal gap is fraught with the possibility of washing a front part of the body surface with the flow even under small deviation of the body axis from the movement direction, and, as a result, with the loss of stability. A finite gap is less advantageous in terms of energy, but it provides steadiness. Advantages and disadvantages of both variants show the expediency of investigating a lateral motion for each of the variants. The peculiarities of impact interaction between the body and the surface of the cavity with a small and sizable gap require development of relevant approaches to the solution of the problem for each of the cases. The difference between the approaches is determined by the natural assumptions, which are valid for each of them. Hence, if the gap between the body and the surface of the cavity is small, the contact area appearing at the instant of impact will be curvilinear, comparable to the specific cross-dimension of the cavity, and developing from the point of initial contact to certain final dimensions corresponding to the maximal body penetration into the fluid. For an extreme case, based on the assumption that the gap dimension is negligibly small, the surface of the contact is constant and takes up half of the cavity cross-section. Finally, in the case when radius of the body cross-section differs from the radius of the cavity cross-section by a certain finite quantity, the contact area is small, compared to relevant dimension of the problem; its curvature is also small, and it can be treated as flat.

Considering these factors, we develop various approaches depending on the dimension of the gap between the body surface and the cavity surface at rest.

3. Small gap case

If the gap d between the cavity and the body at rest is small, but is not equal to zero, the area of the body-fluid contact which appears in the process of impact will not be small. Additionally, it is obvious that the contact area will be variable in a time curvilinear surface.

First, let as present the solution of a supplementary problem for the wave equation (2.2), which allows one to connect the pressure and velocity of the motion on the surface of the cavity. Let us assume that, on this surface, the pressure is given in the form of certain function $P(t,\theta)$:

$$-\left.\frac{\partial\varphi}{\partial t}\right|_{r=1} = P(t,\theta). \tag{3.1}$$

Let us also suppose, that function $P(t,\theta)$ is represented by the Fourier series

$$P(t,\theta) = \sum_{n=0}^{\infty} P_n(t)\cos n\theta, \tag{3.2}$$

and the initial conditions are zero. To solve the given problem, a Laplace integral transformation with respect to t with parameter s is applied to Eq. (2.2) (Bateman and Erdelyi, 1954). The corresponding transforms (images) we denote by the superscript L:

$$f^L(s) = \int_0^{\infty} \mathrm{e}^{-st} f(t)\,dt.$$

Equation (2.2), due to zero initial conditions (2.7), has the following form in image space:

$$\frac{\partial^2\varphi^L}{\partial r^2} + \frac{1}{r}\frac{\partial\varphi^L}{\partial r} + \frac{1}{r^2}\frac{\partial^2\varphi^L}{\partial\theta^2} - s^2\varphi^L = 0, \tag{3.3}$$

and its general solution, with dissipation at infinity (requirement (2.6)), is (Morse and Feshbach, 1953)

$$\varphi^L = \sum_{n=0}^{\infty} A_n(s)\mathrm{K}_n(sr)\cos n\theta. \tag{3.4}$$

Here, $\mathrm{K}_n(sr)$ are McDonald cylindrical functions of an imaginary argument (Bateman and Erdelyi, 1953), and A_n are undefined coefficients.

The pressure and the velocity of the fluid movement can be presented in the form of a Fourier series

$$p(t,\theta) = \sum_{n=0}^{\infty} p_n(t)\cos n\theta, \quad V(t,\theta) = \sum_{n=0}^{\infty} V_n(t)\cos n\theta. \tag{3.5}$$

Then, from the boundary condition (3.1) we obtain a Fourier series component for the image of velocity on the surface of the fluid will be of the form

$$V_n^L(s) = -P_n^L(s)\frac{\mathrm{K}_n'(s)}{\mathrm{K}_n(s)}, \tag{3.6}$$

where $\mathrm{K}_n'(s) = \left[\frac{\partial}{\partial r}\mathrm{K}_n(sr)\right]_{r=1}$. This expression can be modified as follows:

$$V_n^L(s) = -P_n(s)\frac{\mathrm{K}_n(s) - \mathrm{K}_n(s) + \mathrm{K}_n'(s)}{\mathrm{K}_n(s)},$$

or

$$V_n^L(s) = P_n^L(s) - P_n^L(s)R_n^L(s),$$

where

$$R_n^L(s) = -\frac{\mathrm{K}_n(s) + \mathrm{K}_n'(s)}{\mathrm{K}_n(s)}. \tag{3.7}$$

Applying the convolution theorem of operational calculus (Bateman and Erdelyi, 1954) the expression can be rewritten in the original space as follows:

$$V_n(t) = P_n(t) + \int_0^t P_n(\tau) R_n(t-\tau)\,\mathrm{d}\tau, \tag{3.8}$$

where $R_n(t)$ is the original form of the function $R_n^L(s)$—see (3.7), the determination of which is presented in Appendix A. The relation (3.8) allows us to determine the movement velocity of the cavity surface, if pressure is given on this surface:

$$V(t) = P(t) + \sum_{n=0}^{\infty} \int_0^t P_n(t) R_n(t-\tau)\, d\tau \cos n\theta. \tag{3.9}$$

The obtained solution of the supplementary problem is used for the solution of the original mixed problem. From boundary conditions (2.3) and (2.5), and using expressions (3.5) and (3.8), we obtain

$$\sum_{n=0}^{\infty} p_n(t) \cos n\theta + \sum_{n=0}^{\infty} \int_0^t p_n(\tau) R_n(t-\tau)\, d\tau \cos n\theta = v_0(t) \cos\theta, \quad |\theta| < \theta^*,$$

$$\sum_{n=0}^{\infty} p_n(t) \cos n\theta = 0, \quad |\theta| > \theta^*,$$

or making it more compact,

$$\sum_{n=0}^{\infty} p_n(t) \cos n\theta = H(\theta^* - |\theta|) \left[v_0(t) \cos\theta - \sum_{n=0}^{\infty} \int_0^t p_n(\tau) R_n(t-\tau)\, d\tau \cos n\theta \right], \tag{3.10}$$

where $H(x) = \begin{cases} 1, & x > 0, \\ 0, & x < 0, \end{cases}$ is the unit Heaviside function.

The right-hand side of the expression (3.10) as a function of angle variable θ can be presented in the form of a Fourier series. Then, taking into account the orthogonality of the Fourier series and uniqueness of the expansion, it is possible to equate the coefficients of equal harmonics of the left- and right-hand parts. As a result, for the determination of unknown coefficients of Fourier series for pressure on the cavity surface, we have a resolving infinite system of integral Volterra equations of the second kind

$$p_n(t) = v_{0n}(t) - \sum_{m=0}^{\infty} \beta_{mn}(\theta^*) \int_0^t p_m(\tau) R_m(t-\tau)\, d\tau, \quad n = 0, 1, \ldots, \infty, \tag{3.11}$$

with

$$v_{0n}(t) = \frac{v_0(t)}{\pi}\, \vartheta_n, \tag{3.12}$$

$$\vartheta_n = \begin{cases} \sin\theta^*, & n = 0; \\ \theta^* + \dfrac{\sin 2\theta^*}{2}, & n = 1; \\ \dfrac{\sin(n+1)\theta^*}{n+1} + \dfrac{\sin(n-1)\theta^*}{n-1}, & n > 1, \end{cases}$$

$$\beta_{mn}(\theta^*) = \begin{cases} \dfrac{\theta^*}{\pi}, & n = m,\ n = 0; \\ \dfrac{\sin m\theta^*}{\pi m}, & m \neq 0,\ n = 0; \\ \dfrac{1}{\pi}\left(\theta^* + \dfrac{\sin 2m\theta^*}{2m}\right), & n = m,\ n \neq 0; \\ \dfrac{1}{\pi}\left(\dfrac{\sin(n+m)\theta^*}{n+m} + \dfrac{\sin(m-n)\theta^*}{m-n}\right), & n \neq m,\ n \neq 0. \end{cases} \tag{3.13}$$

Thus, the solution of the system (3.11) allows us to calculate the pressure on the cavity surface. The velocity of surface motion is calculated by means of formulas (3.8) or (3.9). Note that the system (3.11) should be solved jointly with

condition (2.10) and the equation of body movement, which in this case has the form

$$\mu\frac{dv_0(t)}{dt}=-\frac{1}{\pi}\sum_{n=0}^{\infty}p_n(t)\vartheta_n,\quad v_0(0)=v_0. \tag{3.14}$$

In conclusion, it is necessary to mention that, for the development of the infinite system of equations of the form (3.11), one can use the solution of the other subsidiary problem, if, unlike the expression (3.1), pressure is given at the cavity surface:

$$\left.\frac{\partial\varphi}{\partial r}\right|_{r=1}=V(t,\theta),\quad V=\sum_{n=0}^{\infty}V_n(t)\cos n\theta. \tag{3.15}$$

The solution of boundary problem (3.15) allows one to obtain coefficients of the Fourier series for the pressure through coefficients $V_n(t)$ in the following form:

$$P_n(t)=V_n(t)+\int_0^t V_n(\tau)\bar{R}_n(t-\tau)\,d\tau,$$

where the kernel $\bar{R}_n(t)$ is determined as the original of the expression

$$\bar{R}_n^L(s)=-\frac{\mathrm{K}_n(s)+\mathrm{K}_n'(s)}{\mathrm{K}_n'(s)}.$$

Correspondingly, the pressure is determined through velocity $V(t,\theta)$ with the expression

$$P(t)=V(t)+\sum_{n=0}^{\infty}\int_0^t V_n(\tau)\bar{R}_n(t-\tau)\,d\tau\cos n\theta. \tag{3.16}$$

Expression (3.15), used together with the expression (2.5) and satisfying mixed boundary conditions (2.3), (2.5), for determination of the coefficients $V_n(t)$, allows one to obtain the infinite system of Volterra integral equations of the second kind

$$V_n(t)=v_{0n}(t)-\sum_{m=0}^{\infty}\bar{\beta}_{mn}(\theta^*)\int_0^t V_m(\tau)\bar{R}_m(t-\tau)\,d\tau,\quad n=0,1,\ldots,\infty. \tag{3.17}$$

Kernel $\bar{R}_n(t)$ and coefficients $v_{0n}(t)$, $\bar{\beta}_{mn}(\theta^*)$ are calculated according to a scheme, analogous to the one presented previously for the infinite system (2.11), which is why we omit the details of the procedure here.

4. Zero gap case

In this section we assume that the difference between the radii of the cavity and the body is so small that it is possible to consider them equal ($d=0$). In this case, it is obvious that polar angle θ^*, defining the boundary of the free surface, is constant and equal to $\theta^*=\pi/2$ (here it is necessary to recall the small depth of penetration). The problem definition and its rigorous solution for zero gap d follows from the relations of previous paragraph, where it is assumed everywhere that $\theta^*=\pi/2$. Then, the resolving infinite system of Volterra integral equations of the second kind is

$$p_n(t)=v_{0n}(t)-\sum_{m=0}^{\infty}\beta_{mn}\int_0^t p_m(\tau)R_m(t-\tau)\,d\tau,\quad n=0,1,\ldots, \tag{4.1}$$

where

$$v_{0n}=v_0(t)\xi_n, \tag{4.2}$$

$$\xi_n=\begin{cases}\dfrac{1}{\pi}, & n=0;\\[2mm] \dfrac{1}{2}, & n=1;\\[2mm] \dfrac{1}{\pi}\left(\dfrac{\sin(n+1)\frac{\pi}{2}}{n+1}+\dfrac{\sin(n-1)\frac{\pi}{2}}{n-1}\right), & n>1;\end{cases}$$

$$\beta_{mn}=\begin{cases}\dfrac{\sin\dfrac{\pi m}{2}}{\pi m}, & m\neq 0,\ n=0;\\ \dfrac{1}{2}, & n=m;\\ \dfrac{1}{\pi}\left(\dfrac{\sin(m+n)\dfrac{\pi}{2}}{m+n}+\dfrac{\sin(m-n)\dfrac{\pi}{2}}{m-n}\right), & n\neq m,\ n\neq 0.\end{cases} \tag{4.3}$$

System (3.1) is solved together with the equation of body motion

$$\mu\frac{dv_0(t)}{dt}=-\frac{F(t),}{\pi}\quad v_0(0)=v_0,$$
$$F(t)=\pi\sum_{n=0}^{\infty}p_n(t)\xi_n. \tag{4.4}$$

Functions $R_n(t)$, $n=0,1,\ldots$, are determined by the formulas obtained in Section 3.

Additionally, we propose a more simplified approximate solution, based on two assumptions, which should not considerably distort the initial statement and the results assumed. The first of the suppositions, $\theta^*=\pi/2$, was already mentioned above. Also, we assume, that condition (3.5) on the free surface of the cavity can be substituted (with an error to be estimated later in a rigorous solution of the problem (3.2)–(3.10)) for the condition of its (''rigid screen'' model)

$$\left.\frac{\partial\varphi}{\partial r}\right|_{r=1}=0,\quad |\theta|>\theta^*. \tag{4.5}$$

As a result of the introduced assumptions after the application of Laplace integral transformation in time, the problem is reduced to a solution in the space of images of equation (3.3) with the following boundary condition:

$$\left.\frac{\partial\varphi^L}{\partial r}\right|_{r=1}=\begin{cases}v_0^L(s)\cos\theta & |\theta|<\dfrac{\pi}{2}\\ 0, & |\theta|>\dfrac{\pi}{2}\end{cases} \tag{4.6}$$

As follows from (4.6), the given boundary problem is not mixed anymore. The right-hand side of condition (4.6) can be presented in the form of a Fourier series

$$V^L=H\left(\frac{\pi}{2}-|\theta|\right)v_0^L(s)\cos\theta=\sum_{n=0}^{\infty}v_{0n}^L(s)\cos n\theta,$$
$$v_{0n}^L(s)=\xi_n v_0^L(s). \tag{4.7}$$

Here, $H(x)$ is the unit Heaviside function. Substituting solution (3.5) into the condition (4.6), we obtain for each n

$$A_0=\frac{v_0^L(s)}{\pi s\mathrm{K}_0'(s)},\quad A_1=\frac{1}{2}\frac{v_0^L(s)}{s\mathrm{K}_1'(s)};$$
$$A_n=\xi_n\frac{v_0^L(s)}{s\mathrm{K}_n'(s)},\quad n=2,\ldots,\infty,\quad \mathrm{K}_n'(x)=\frac{\partial}{\partial x}\{\mathrm{K}_n(x)\},$$

from which the pressure on the cavity surface is determined, as follows:

$$p(t)=\sum_{n=0}^{\infty}p_n(t)\cos n\theta,\quad p_0^L(s)=-\frac{1}{\pi}v_0^L(s)\frac{\mathrm{K}_0(s)}{\mathrm{K}_0'(s)};$$
$$p_1^L(s)=-\frac{1}{2}v_0^L(s)\frac{\mathrm{K}_1(s)}{\mathrm{K}_1'(s)},\quad p_n^L(s)=-\xi_n v_0^L(s)\frac{\mathrm{K}_n(s)}{\mathrm{K}_n'(s)}. \tag{4.8}$$

Again, the problem consists of determination of the originals of functions $p_n^L(s)$, $n=0,1,\ldots,\infty$. For this purpose, we multiply the left-hand and right hand parts of expressions (4.8) by $\mathrm{e}^{-s}\mathrm{K}_n'(s)$, employ recursion formulas (3.15) for representation of $\mathrm{K}_n'(s)$, and apply the convolution theorem of originals to the result. Thereby, we make use of the following tabular correspondence between the image and the original, represented by formulas (A.6). As a result, we

obtain Volterra integral equations of the first kind for determining coefficients $p_n(t)$:

$$\int_0^t p_n(\tau)R_n(t-\tau)\,d\tau = G_n(t), \quad n = 0, 1, \ldots, \infty, \tag{4.9}$$

where kernel $R_n(t)$ is determined on the basis of relations (A.6) as

$$R_n(t) = -\frac{(z_1^n(t) + z_2^n(t))(t+1)}{2\sqrt{t(t+2)}},$$

and the right-hand side $G_n(t)$ represents the convolution of originals of functions $v_0^L(s)$ and $\mathrm{K}_n(s)$

$$G_n(t) = -\xi_n \int_0^t v_0(t-\tau)\frac{z_1^n(\tau) + z_2^n(\tau)}{2\sqrt{\tau(\tau+2)}}\,d\tau. \tag{4.10}$$

Equation (4.7) has a kernel with weak singularity and can be solved numerically, for instance, by reduction to a system of algebraic equations with the help of a method described in Kubenko (1979).

There are other methods for the solution of the conversion problem of expressions of the form (4.8); the problem can be reduced to the solution of a Vorlerra integral equation of the second kind. For this, recalling that at $s \to \infty$ the relation $\mathrm{K}_n(s)/\mathrm{K}_n'(s) \to -1$, expression (4.8) can be rewritten in the form

$$p_n^L \frac{\mathrm{K}_n(s) - \mathrm{K}_n(s) + \mathrm{K}_n'(s)}{\mathrm{K}_n(s)} = -\xi_n v_0^L(s),$$

or

$$p_n^L\left(1 - \frac{\mathrm{K}_n'(s) + \mathrm{K}_n(s)}{\mathrm{K}_n(s)}\right) = \xi_n v_0^L(s). \tag{4.11}$$

The application of the convolution theorem to (4.11) allows one to obtain the following sequence of integral equations:

$$p_n(t) = \xi_n v_0(t) - \int_0^t p_n(\tau)R_n(t-\tau)\,d\tau, \quad n = 0, 1, \ldots, \infty. \tag{4.12}$$

It is clear, that the problem of kernel image conversion still remains, however, the originals of images such as $R_n(s) = -[\mathrm{K}_n'(s) + \mathrm{K}_n(s)]/\mathrm{K}_n(s)$ are much smoother functions, than the originals of fraction $\mathrm{K}_n(s)/\mathrm{K}_n'(s)$, which is present in expressions (4.8), and their extraction should not cause trouble; ways to obtain then will be discussed in the Appendix A.

It is necessary to recall that expressions (4.9) (or (4.12)) should be solved jointly with the equation of the body movement.

In the problem statement with zero gap, some corrections are possible if the polar angle of the contact area θ^* is determined on the basis of the relation (2.10), from which it follows that at $d = 0$

$$\theta^* = \arccos\frac{z^*(t)}{2}. \tag{4.13}$$

In conclusion, it is necessary to mention that the sequence of integral equations (4.12) (realizing the solution of the problem with simplified formulation of boundary conditions (4.6)) is derived in a similar way for small finite gap d and is omitted in this publication for brevity.

5. Asymptotic solution

5.1. Zero gap case

As follows from Section 4, with zero gap in the simplified problem statement, the problem is reduced to the solution of a sequence of Volterra integral equations (4.9) or (4.12) with a differential equation (2.8). An asymptotic solution of this problem for very small interaction time can be determined by use of the asymptotic presentation of cylindrical McDonald functions of large argument (Bateman and Erdelyi, 1953)

$$\mathrm{K}_n(s) \approx \sqrt{\frac{\pi}{2s}}\mathrm{e}^{-s}(1 + \ldots); \quad \mathrm{K}_n'(s) \approx -\sqrt{\frac{\pi}{2s}}\mathrm{e}^{-s}(1 + \ldots), \tag{5.1}$$

which, in accordance with theorem of limiting values of operational calculus, allows one to find the corresponding originals for a small initial time interval. Thus, as is obvious in Eq. (4.8), in the original space, we obtain the relation $p_n(t) = \xi_n v_0(t)$, $n = 0, 1, \ldots, \infty$, from which it follows that

$$p = V = H\left(\frac{\pi}{2} - \theta\right) v_0(t) \cos\theta, \tag{5.2}$$

i.e., the pressure is proportional to the velocity (a well-known relation, which in hydro-elasticity and acoustics is called the hypothesis of a plane wave; it is worth noticing that the given relation is correct only at small values of interaction time). Thus, from the equation of the body motion, we obtain

$$\mu \frac{dv_0(t)}{dt} = -\frac{2v_0(t)}{\pi} \int_0^{\pi/2} \cos^2\theta \, d\theta, \quad v_0(0) = v_0$$

or

$$\mu \frac{dv_0(t)}{dt} = -\frac{v_0(t)}{2}, \quad v_0(0) = v_0. \tag{5.3}$$

The solution of Eq. (5.3) is $v_0(t) = v_0 \, e^{-t/2\mu}$. According to (5.2), the pressure has the same time dependence:

$$p(t) = v_0 \, e^{-t/2\mu} \tag{5.4}$$

Correspondingly, the drag is determined by the formula

$$F(t) = \frac{\pi}{2} v_0 \, e^{-t/2\mu}. \tag{5.5}$$

As it is clear from (5.4), unlike the model of incompressible fluid (which determines the infinitely large value of hydrodynamical pressure at the initial instant of time), the present approach (taking into account fluid compressibility) establishes that the pressure at $t = 0$ has a finite value and decreases with time. It is necessary to remember, however, that the results presented above are obtained via asymptotic relations (5.1), and are correct only on a small time interval, starting from the initial contact moment. In fact, the obtained solution (5.4) and (5.5) does not define the motion of the body during a considerable time interval. Its clarification requires the solution of integral equations (4.7), (or (4.10)) or, even better, the solution of infinite system of Volterra integral equations.

If the boundary of the contact area is determined according to (4.13), the drag can be determined as

$$F(t) = -2v_0(t) \int_0^{\theta^*} \cos^2\theta \, d\theta, \tag{5.6}$$

and for the determination of the penetration velocity, we obtain the system of two differential equations of the 1st order

$$\begin{aligned} &\frac{dz^*(t)}{dt} = v_0(t), \\ &\mu \frac{dv_0(t)}{dt} = -\frac{v_0(t)}{\pi} \left(\arccos\frac{z^*(t)}{2} + \frac{1}{2}\sqrt{1 - \frac{z^*(t)}{4}} \right), \\ &z^*(0) = 0, \quad v_0(0) = v_0. \end{aligned} \tag{5.7}$$

5.2. Small nonzero gap case

If asymptotic expressions (5.1) are applied to relations (3.6), we again obtain the equality $p_n(t) = V_n(t)$, $n = 0, 1, \ldots$ from which follows (5.2). Then, the hydrodynamic force is

$$F(t) = 2v_0(t) \int_0^{\theta^*} \cos^2\theta \, d\theta,$$

or

$$F(t) = v_0(t)\left(\theta^* + \frac{\sin 2\theta^*}{2}\right), \quad \theta^* = \arccos\left(\frac{(z^*)^2 + 2d(z^* + 1)}{2(d + z^*)}\right), \tag{5.8}$$

and the penetration velocity is determined from the system of differential equations

$$\frac{dz^*(t)}{dt} = v_0(t), \quad \mu\frac{dv_0(t)}{dt} = -\frac{v_0(t)}{\pi}\left(\theta^* + \frac{1}{2}\sqrt{1-\frac{\theta^{*2}}{4}}\right),$$
$$z^*(0) = 0, \quad v_0(t) = v_0. \tag{5.9}$$

5.3. Finite gap case

If the boundary of the fluid is plane, then it is obvious that

$$x^* = \sin\theta^* = \sin\arccos(1 - z^*(t)) = \sqrt{2z^*(t) - (z^*(t))^2}.$$

For the early stage of interaction, using the asymptotic relations of cylindrical functions, we can obtain relation (5.2), and the expression for the drag will be of the form

$$F(t) = 2v_0(t)\int_0^{x^*} \cos^2 x\,dx, \quad x^* = \sqrt{2z^*(t) - (z^*(t))^2}.$$

Then, for determination of the penetration velocity, we obtain the following system of equation

$$\frac{dz^*(t)}{dt} = v_0(t),$$
$$\mu\frac{dv_0(t)}{dt} = -\frac{v_0(t)}{\pi}\left(\sqrt{2z^*(t) - (z^*(t))^2} + \frac{1}{2}\sin 2\left(\sqrt{2z^*(t) - (z^*(t))^2}\right)\right),$$
$$z^*(0) = 0, \quad v_0(0) = v_0. \tag{5.10}$$

Thus, systems of differential equations (5.3), (5.7), (5.9), (5.10) allow one to calculate the velocity of movement and the hydrodynamic force at the earliest stages of penetration, with different characteristic ratios between the radius of the body and radius of the cavity.

6. Numerical solution

The research on the impact process in the general statement is reduced to a joint solution of the infinite system (sequence) of linear Volterra integral equations of the second kind, (3.11), (4.1) or (4.12), a differential equation of motion (2.8) similar to (3.14), and relation (2.10) specifying the boundary of the contact area.

The solution of the problem was realized numerically on a finite time interval $[0,T]$, divided into equal parts with step Δt, and at partition nodes, the required quantities were calculated.

The infinite system (sequence) of integral equations (3.11), (4.1), (4.12), and right-hand side of differential equation (3.14) were subjected to reduction. The order of reduction N was chosen from the point of view of practical convergence of the solution. All integrals were calculated by quadratic formulas of left rectangles. As a result, the given system is reduced to a system of algebraic equations. Differential equation (3.14) is replaced with the difference equation. For improvement of convergence of the Fourier series, Gibbs σ-multipliers were applied

$$\sigma_n = \begin{cases} 1, & n = 0; \\ \dfrac{\sin\dfrac{\pi n}{N}}{\dfrac{\pi n}{N}}, & n = \overline{1,N}. \end{cases} \tag{6.1}$$

Kernel $R_n(t)$ of the infinite system (sequence) of integral equations (4.1), (4.12) is determined from (A.4), where function $R_{n1}(t)$ satisfies the Volterra equation of the first kind (A.7). For its calculation, the following approach was applied: (i) the interval of integration was divided into equal small segments $[t_j; t_{j+2}]$, $j = 0, 2, \ldots M-2$; (ii) every integral was substituted for the sum of integrals by the segment of partition $[t_j; t_{j+2}]$; (iii) value $R_{n1}(t)$ on each interval $[t_j; t_{j+2}]$ was assumed constant and was taken outside the integral sign with the value of $R_{n1}(t_{j+1})$; (iv) integrals $\int_{t_j}^{t_{j+2}} G_n(t-\tau)\,d\tau$ were calculated analytically; (v) as a result of this procedure, Eq. (16) is reduced to a system of linear algebraic equations with respect to $R_{n1}(t_k)$ with a triangular matrix, where $k \in \left(0; \frac{M}{2}\right)$.

7. Analysis of the results

In calculations in the interval of time [0;4] the following parameters were modified: the dimensionless linear mass of a body $\mu = 0.25$–20 and ∞ (the motion of the body with constant velocity corresponds to value of $\mu \to \infty$); initial velocity of penetration $v_0 = 0.01$–0.05, gap between the cavity and the body $d = 0.2$–1.

In Fig. 3, time dependence of hydrodynamic pressure $p(t)$ at the frontal point at different values of the linear mass of the cylinder is shown ($\mu = 0.5$, 1, 2 and ∞, initial velocity $v_0 = 0.05$, value of the gap between the cavity and the body $d = 0.2$).

Fig. 3 shows that the hydrodynamic pressure in the frontal point of the body at time instant $t = 0$, in accordance with the hypothesis of a plane wave, is equal to its maximal value of $p = \rho C v_0$ in dimensional notation. Further, at the initial stage of the considered time interval, the pressure abruptly falls, and the lighter is the body, the quicker the fall.

Fig. 4 illustrates the time dependence of hydrodynamic pressure at the frontal point for various values of gap $d = 0.2$, 0.4 and 0.7 (initial velocity $v_0 = 0.05$, and the mass of the body $\mu = 4$).

In Fig. 4, we notice that the smaller the gap d, the bigger the hydrodynamic pressure at the frontal point.

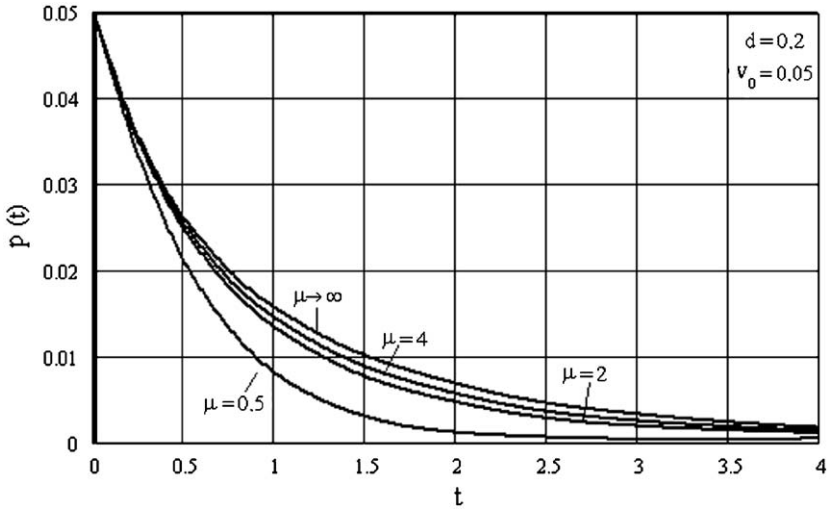

Fig. 3. Time dependence of hydrodynamic pressure in frontal point for various μ values.

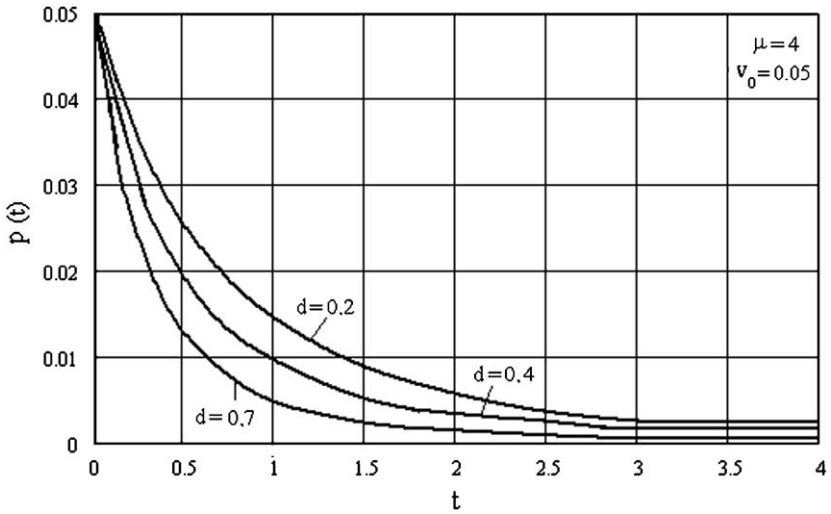

Fig. 4. Time dependence of hydrodynamic pressure in frontal point for various d values.

Fig. 5 depicts the dependence of the drag $F(t)$ on time for velocity $v_0 = 0.05$ and gap $d = 0.2$, with various values of mass $\mu = 0.5$, 2, 4 and ∞.

Fig. 5 shows that

(i) the larger value of μ at the arbitrary time instant is associated with the larger value of the hydrodynamic force;
(ii) the hydrodynamic force on the considered interval of time attains its maximal value. The maximal value attains quicker if the body is easier one.

Fig. 6 shows the dependence of the drag $F(t)$ on time for velocity $v_0 = 0.05$, mass $\mu = 4$, for various values of gap $d = 0.01$, 0.05 and 0.2. In Fig. 6, one can see that the larger value of d at an arbitrary time instant is associated with the smaller value of the drag.

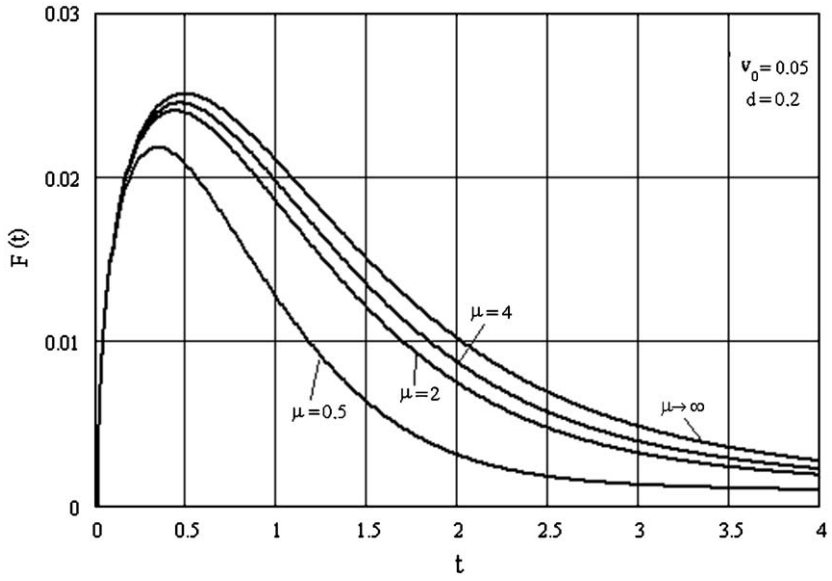

Fig. 5. Dependence of the drag on time for various values of μ.

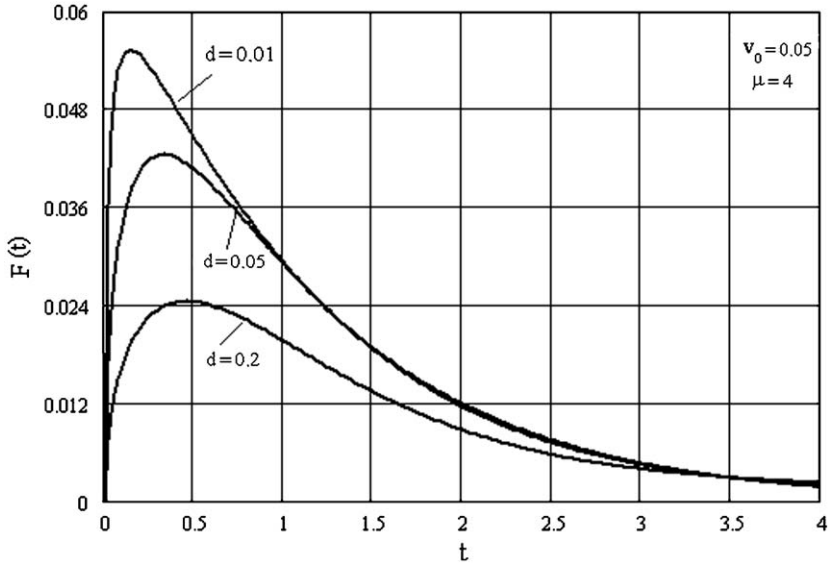

Fig. 6. Dependence of the drag on time for various values of d.

Fig. 7 presents the comparison of values of the drag $F(t)$ on time interval [0;10] at the penetration of the cylindrical body with constant velocity v_0 through the surface of the cavity. The values were obtained by the use of various models of fluid; in the present publication, we have a compressible fluid model, while in the paper by Paryshev (2003), we see an incompressible fluid model. In the calculations, the following values for parameters were used: $\mu \to \infty$, $v_0 = 0.01$, $d = 0.01$ (in the case of small gap). Curves, marked in the figures as 1 and 2, correspond to the models of compressible and incompressible fluid, accordingly.

In Fig. 8, an analogous comparison of values of the drag $F(t)$ on the time interval [0;10] at penetration of cylindrical body with constant velocity v_0 through the cavity surface is shown for the gap $d = 0.2$.

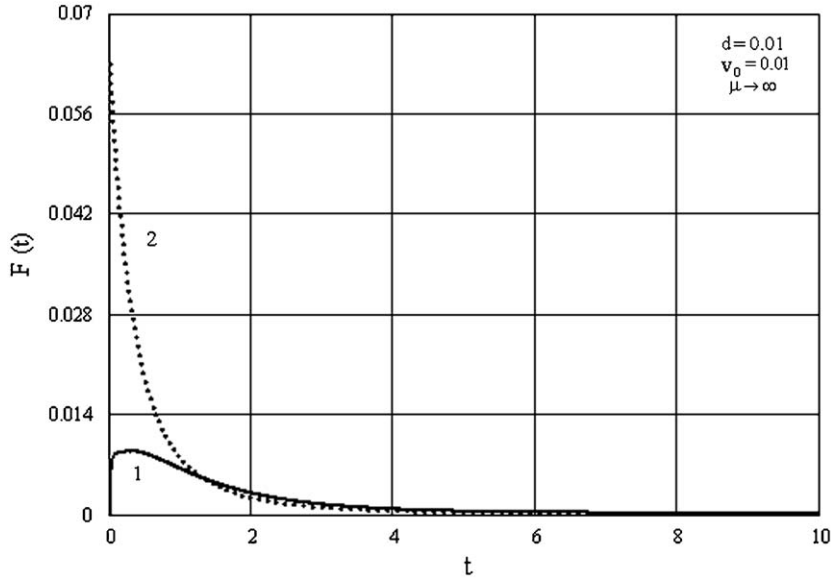

Fig. 7. Comparison of the results obtained for the drag with the use of models of compressible and incompressible fluid ($d = 0.01$, $v_0 = 0.01$).

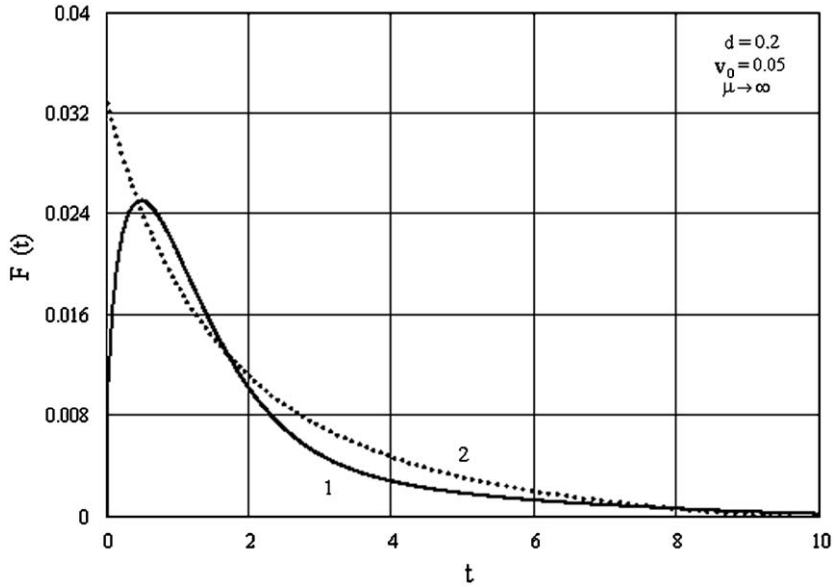

Fig. 8. Comparison of the results obtained for the drag with the use of models of compressible and incompressible fluid ($d = 0.20$, $v_0 = 0.05$).

Figs. 7 and 8 demonstrate that: (i) the value of hydrodynamic force for the case of an incompressible fluid (Curve 2) at the initial moment of time has a finite jump, and in the case of an compressible fluid (Curve 1), the curve starts from zero and accomplishes its maximal value at a certain moment of time; this moment occurs later if the gap is larger and it can continue for 1–3 time units; (ii) a the later stages, both models allow one to obtain results with close values.

Fig. 9 shows the time dependence of motion velocity $v_0(t)$ for the initial value $v_0 = 0.05$, gap $d = 0.2$, values of mass $\mu = 0.5$, 2, 4 and ∞. It is shown, that the velocity of the cylinder motion essentially depends on its mass; the more massive is the body, the bigger the velocity.

Fig. 10 represents the time dependence of motion velocity $v_0(t)$ for various values of gap $d = 0.2$, 0.4 and 0.7, if initial velocity is $v_0 = 0.05$, and mass $\mu = 0.5$.

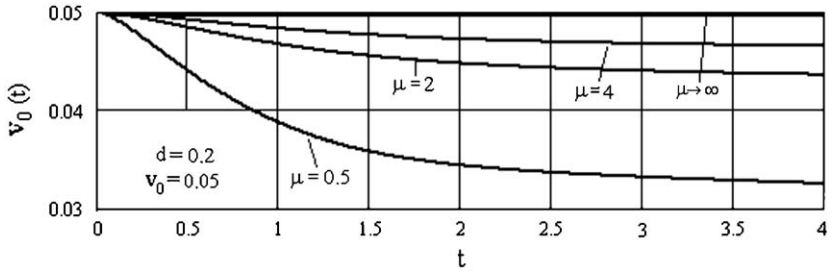

Fig. 9. Time dependence of motion velocity, for various values of μ.

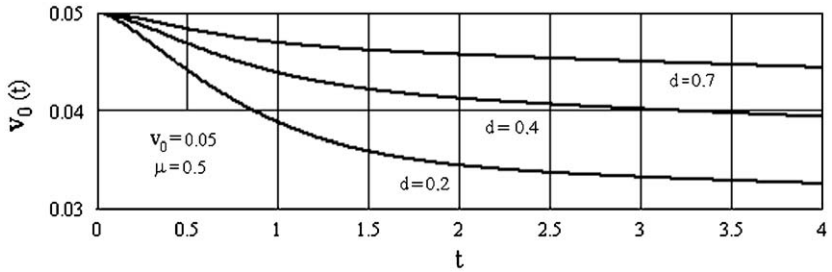

Fig. 10. Time dependence of motion velocity, for various values of d.

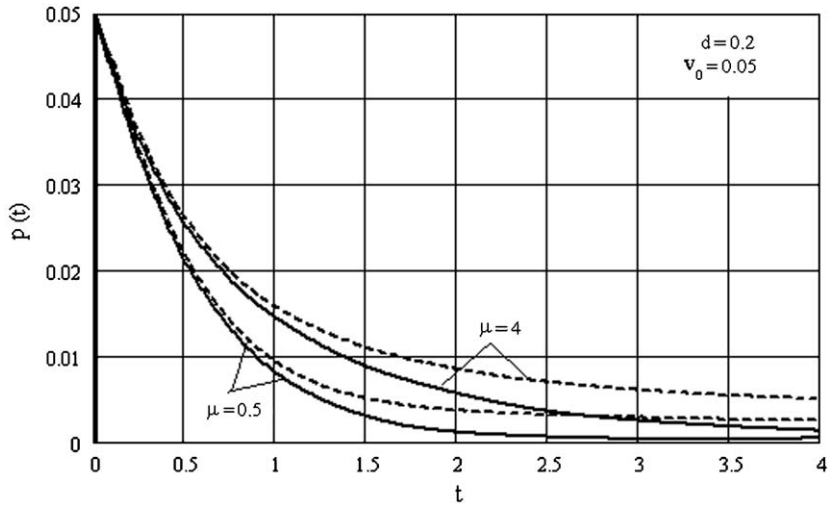

Fig. 11. Comparison of the results obtained for the pressure with the use of "general" and "rigid screen" statements.

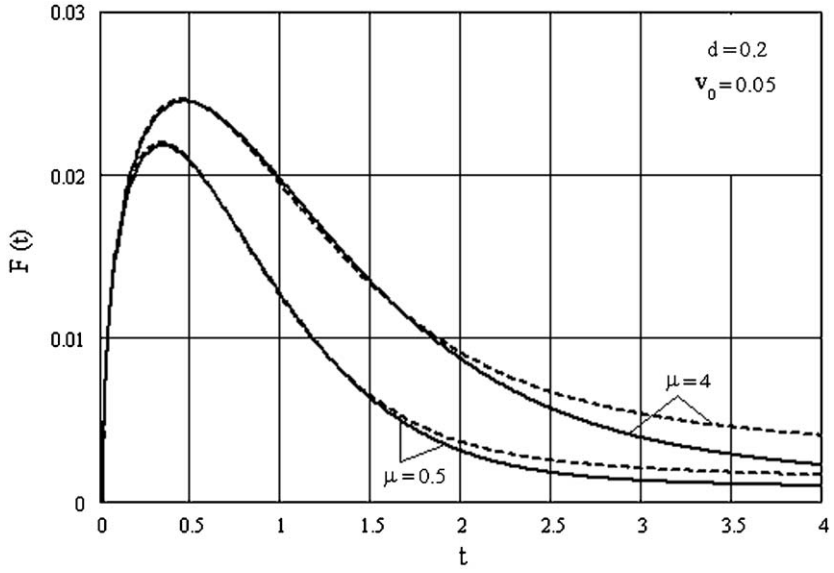

Fig. 12. Comparison of the results obtained for the drag with the use of ''general'' and ''rigid screen'' statements.

Fig. 10 demonstrates that the larger values of the gap corresponds to the larger values of velocity of the body motion. The explanation is that with the growth of gap d, the drag preventing the penetration of the body decreases (see Fig. 6).

Fig. 11 shows a comparison of results for hydrodynamic pressure $p(t)$, obtained on time interval [0;4] with the use of various statements: the ''rigid screen'' model and the ''general'' statement with natural boundary conditions on the free surface of the cavity. The following values for parameters were used in calculations: initial velocity $v_0 = 0.05$, gap $d = 0.2$, linear mass $\mu = 0.5$ and 4. The curves, marked with a dotted line and firm line on the figure, correspond to the ''rigid screen'' model and to the ''general'' statement, accordingly.

Fig. 12 depicts comparison of the results of calculations for hydrodynamic force $F(t)$ for various statements, the ''rigid screen'' model and ''general'' statement. The following values of parameters were used in calculations: initial velocity $v_0 = 0.05$, gap $d = 0.2$, linear mass $\mu = 0.5$ and 4. The curves, marked in the picture with dotted and firm lines, correspond to the ''rigid screen'' model and to the ''general'' statement.

From Figs. 11 and 12, it is obvious that more ''rigorous'' conditions on the free surface of the cavity raise the values of the hydrodynamic loadings by too much, but as far as this difference in the values of characteristics is insignificant, we can recommend the given simplified technique for obtaining an engineering evaluation of process development in order to considerably reduce the use of computer time.

Fig. 13 illustrates the distribution of hydrodynamic pressure $p(t)$ on the surface of the cavity at time $t = 0.5$ and 1.5 at various values of gap $d = 0.2$ and 0.4, for values of initial velocity $v_0 = 0.05$ and mass $\mu = 4$. From Fig. 13, it follows, that on the considered interval of time, the smaller is the value of gap d, the higher the pressure within the bounds of the contact area and the bigger the contact area itself.

Fig. 14 represents a comparison of numerical and asymptotical results obtained with the use of a ''rigid screen'' statement for hydrodynamic force $F(t)$ with zero gap. The values for parameters used in calculations were $\mu = 4$, $v_0 = 0.001$. Curves, marked with dotted and continuous lines in the figure correspond to numerical and analytical solutions, accordingly.

Fig. 15 shows the comparison of numerical and analytical (asymptotical) results obtained with the use of the ''rigid screen'' statement for the velocity of cylinder motion $v_0(t)$ for zero gap. The values for the parameters that were used in calculations are the same: $\mu = 4$ and $v_0 = 0.001$. Curves, marked with dotted and firm lines in the figure, correspond to numerical and analytical results.

Fig. 16 illustrates the comparison of the numerical and analytical results, obtained on time interval [0;1] for hydrodynamic force $F(t)$ with the small gap. In calculations, we used the following values for parameters: $\mu \to \infty$, $d = 0.01$, $v_0 = 0.05$. Curves, marked with dotted and continuous lines in the figure, correspond to numerical and asymptotical results.

From Figs. 14–16, it is obvious that the results obtained asymptotically, are somehow too high for hydrodynamic loadings and are too low for kinematic ones in comparison with similar numerical results. Taking into account the fact

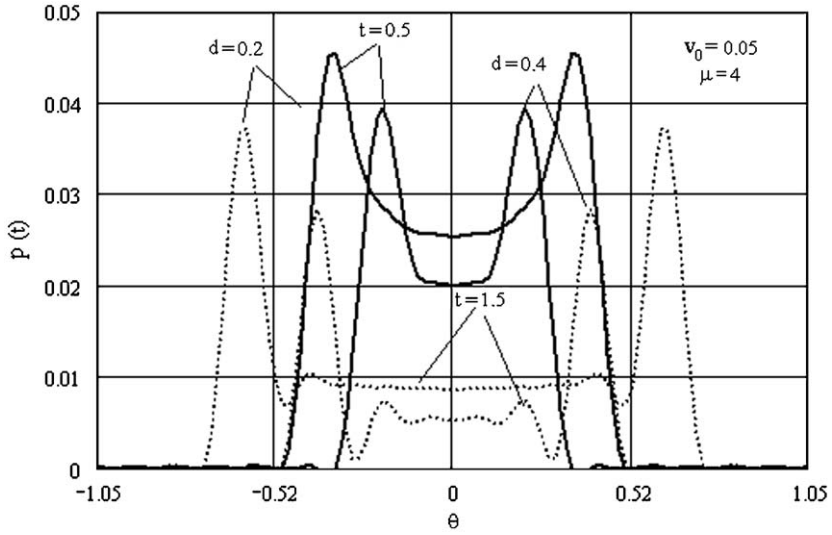

Fig. 13. The pressure distribution on the wetted surface of the cylinder.

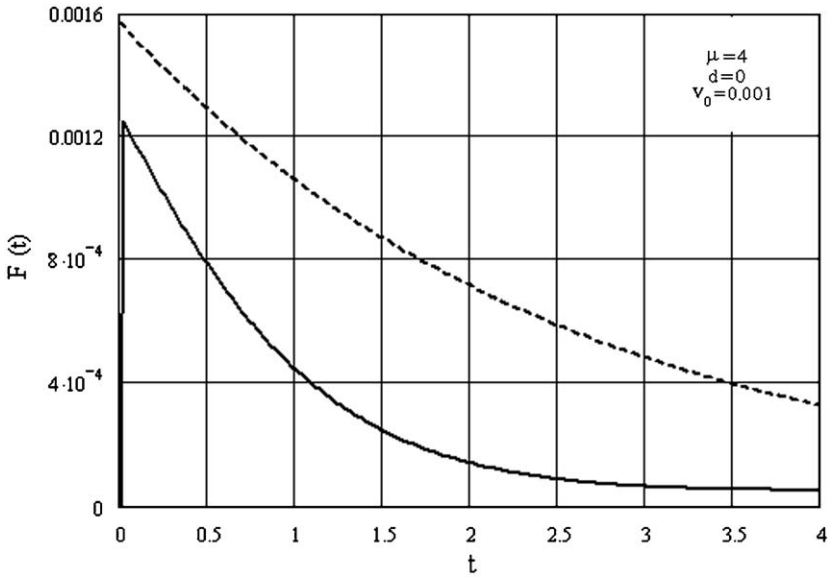

Fig. 14. Zero gap: comparison of numerical and asymptotical results obtained for the drag.

that the difference in values of given characteristics is insignificant, we can obtain fast evaluation of process development, by taking into account the safety margin of construction. It is also possible to recommend the given simplified technique of solution of the impact interaction problem between the body and the surface of the cavity, since it will considerably reduce waste of computer time.

6. Conclusions

The approach, developed in the present study allows one to investigate (within the framework of a plane problem) the process of impact interaction between a thin long cylindrical body and the surface of the cylindrical cavity in an ideal compressible fluid. Various modifications of the approach are provided depending on the ratio of specific values of the cross-section of the body and the cavity. In all cases the mixed (or non-mixed) non-stationary boundary value problem

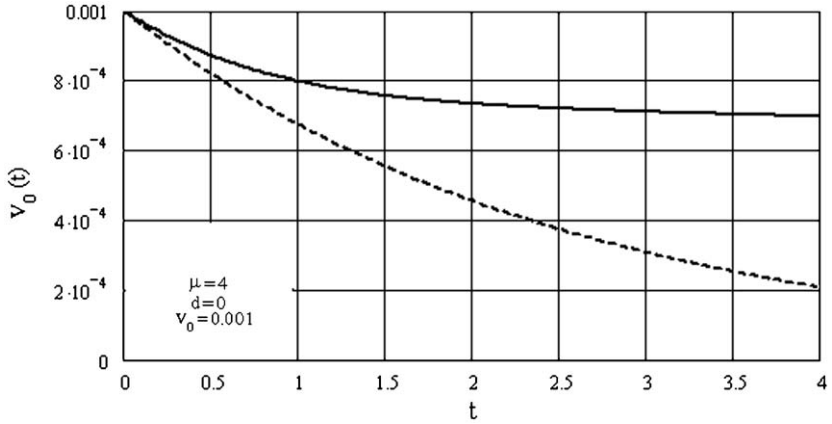

Fig. 15. Zero gap: comparison of numerical and asymptotical results obtained for the velocity.

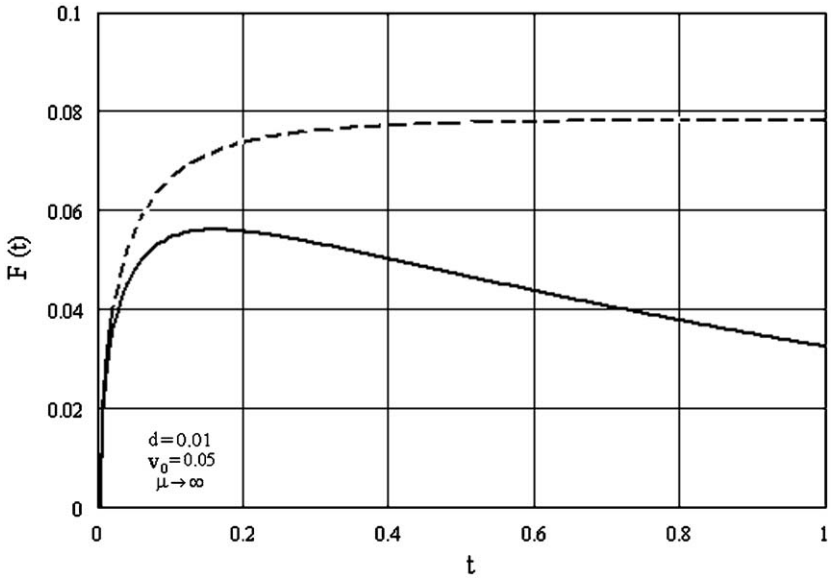

Fig. 16. Small gap: comparison of numerical and asymptotical results obtained for the drag.

with the moving unknown (or known) boundary is formulated, the solution of which, by decomposing the required quantities in Fourier series and application of the obtained solution of a supplementary problem (Laplace integral transformation in time is used), is reduced to the solution of the infinite system (sequence) of Volterra integral equations of the second kind. The given system is a part of the general bound resolving system of equations, also containing the equation of lateral motion of a body and the relation which defines the boundaries of the contact area. Both approximate-asymptotic and numerical solutions for the initial stage of interaction are obtained. The comparison of asymptotic and numerical solutions shows their qualitative correspondence. The evaluation of the degree of boundary conditions on the free surface of cavity affecting the sought characteristics has been carried out. The use of the compressible fluid model allows one to obtain results more adequate to the physics of the process at an early stage of the body-liquid interaction.

Appendix A

While constructing resolving system (3.11), we omitted the issue of calculation of integral operator kernel—function $R_n(t)$, $n = 0, 1, \ldots$,—whose Laplace transform is given by the formula (3.7).

Here, we represent an example of the solution of such a non-trivial problem. For this, we shall use the asymptotical presentation of a McDonald function of large argument (Bateman and Erdelyi, 1954) of the form:

$$\mathrm{K}_n(S) \approx \sqrt{\frac{\pi}{2s}}\mathrm{e}^{-s}\left(1+\frac{4n^2-1}{8s}+\cdots\right), \quad \mathrm{K}_n'(s) \approx -\sqrt{\frac{\pi}{2s}}\mathrm{e}^{-s}\left(1+\frac{4n^2+3}{8s}+\cdots\right). \tag{A.1}$$

The given asymptotic form allows us to easily write first terms of the asymptotic expansion of function $R_n^L(s)$:

$$R_n^L(s) \approx -\frac{\frac{1}{2s}\mathrm{e}^{-s}\sqrt{\frac{\pi}{2s}}}{\sqrt{\frac{\pi}{2s}}\mathrm{e}^{-s}\left(1+\frac{4n^2-1}{8s}+\cdots\right)} \approx \frac{1}{2s}\left(1-\frac{4n^2-1}{8s}+\cdots..\right) = \frac{1}{2s}-\frac{(4n^2-1)}{16s^2}-\cdots.$$

If, in expression (3.7), we select the obtained dominant term of the asymptotic expansion, and additionally use the recurrence relations for cylindrical functions of the following form:

$$\begin{aligned} &-2n\mathrm{K}_n(z) = z\mathrm{K}_{n-1}(z) - z\mathrm{K}_{n+1}(z), \quad \frac{d}{dz}\mathrm{K}_n(z) = -\mathrm{K}_{n-1}(z) - \frac{n}{z}\mathrm{K}_n(z), \\ &\frac{d}{dz}\mathrm{K}_n(z) = -\mathrm{K}_{n+1}(z) + \frac{n}{z}\mathrm{K}_n(z), \end{aligned} \tag{A.2}$$

we obtain

$$\begin{aligned} R_n^L(s) &= \frac{1}{2s} - \frac{\left(n+\frac{1}{2}\right)\frac{1}{s}\mathrm{K}_n(s) + \mathrm{K}_n(s) - \mathrm{K}_{n+1}(s)}{\mathrm{K}_n(s)} = \frac{1}{2s} + R_{n1}^L(s), \\ R_{n1}^L(s) &= -\frac{\left(n+\frac{1}{2}\right)\frac{1}{s}\mathrm{K}_n(s) + \mathrm{K}_n(s) - \mathrm{K}_{n+1}(s)}{\mathrm{K}_n(s)}. \end{aligned} \tag{A.3}$$

Then

$$R_n(t) = \frac{1}{2}H(t) + R_{n1}(t), \tag{A.4}$$

where function $R_{n1}(t)$ is quite a smooth function (since, according to formula (4.18), from function $R_n(t)$, the step part is singled out). Now we need to determine the function $R_{n1}(t)$. For this purpose, we re-write the second of Eqs. (A.3) as follows:

$$\mathrm{e}^s\mathrm{K}_n(s)R_{n1}^L(s) = -\mathrm{e}^s\left[\left(n+\frac{1}{2}\right)\frac{1}{s}\mathrm{K}_n(s) + \mathrm{K}_n(s) - \mathrm{K}_{n+1}(s)\right]. \tag{A.5}$$

For the conversion of the expression (A.4) with respect to the Laplace transform we make use of the theorem of operational calculation convolution (Bateman and Erdelyi, 1954). Here, the conversion of the McDonald function can be found with the help of relations (Bateman and Erdelyi, 1954; Kubenko, 1979)

$$\begin{aligned} &\mathrm{e}^s\mathrm{K}_n(s) \leftrightarrow \frac{z_1^n + z_2^n}{2Z}; \quad \frac{\mathrm{e}^s}{s}\mathrm{K}_0(s) \leftrightarrow \ln z_1; \quad \frac{\mathrm{e}^s}{s}\mathrm{K}_n(s) \leftrightarrow \frac{z_1^n - z_2^n}{2n}, \\ &z_{1,2}(t) = t + 1 \pm Z, \quad Z = \sqrt{(t+1)^2 - 1}. \end{aligned} \tag{A.6}$$

Thus, for determination of functions $R_{n1}(t)$, we obtain a Volterra integral equation of the first kind

$$\int_0^t R_{n1}(\tau)G_n(t-\tau)\,d\tau = g_n(t), \quad n = 0, 1, 2, \ldots \tag{A.7}$$

The kernel and the right-hand side have the form:

$$G_n(t)=\frac{z_1^n(t)+z_2^n(t)}{2\sqrt{t(t+2)}};\quad g_0(t)=\frac{t}{\sqrt{t(t+2)}}-\frac{1}{2}\ln(z_1(t));$$
$$g_n(t)=\frac{z_1^n(t)+z_2^n(t)}{2\sqrt{t+2}}\sqrt{t}-\frac{z_1^n(t)-z_2^n(t)}{4n}.$$

Integral equation (A.8) belongs to equations with weak singularity and can be solved numerically, based on the method presented in Kubenko (1979).

Thus, the kernel in the integral operator of the system (3.11) is determined according to formula (A.4) from the solution of a sequence of Volterra integral equations of the first kind (A.7).

For more convenient numerical evaluation, the approximate pattern of kernel definition in a system of Volterra integral equations of the second kind (3.11) can be proposed. With this aim, we use the well-known asymptotic qualities of cylindrical functions of large index (Abramowitz and Stegun, 1964)

$$\mathrm{K}_v(vz)\approx\sqrt{\frac{\pi}{2v}}\frac{\mathrm{e}^{-v\eta}}{(1+z^2)^{1/4}}\{1+\cdots\};\quad \mathrm{K}_v'(vz)\approx-\sqrt{\frac{\pi}{2v}}\frac{(1+z^2)^{1/4}}{z}\,\mathrm{e}^{-v\eta}\{1+\ldots\},$$
$$\eta=\sqrt{1+z^2}+\ln\frac{z}{1+\sqrt{1+z^2}}.$$

Then, for the kernel $R_n(t)$, we have the following asymptotic for large n:

$$R_n^L(s)=-\frac{\mathrm{K}_n'(s)+\mathrm{K}_n(s)}{\mathrm{K}_n(s)}\approx-\left(1-\sqrt{1+\left(\frac{n}{s}\right)^2}\right)=\left(\frac{n}{s}\right)^2\frac{s}{s+\sqrt{s^2+n^2}}.$$

The original-space form of the last expression is easily derived with help of

$$R_n(t)=n\int_0^t\frac{\mathrm{J}_1(n\tau)}{\tau}\,\mathrm{d}\tau. \tag{A.8}$$

Here, $J_1(x)$ is a Bessel cylindrical function (Bateman and Erdelyi, 1953).

Expression (A.8) can be used with sufficiently large n. At small values of n, it is necessary to use the relations (A.4) and (A.7) or to apply rational approximations to the presentation of McDonald cylindrical functions (Abramowitz and Stegun, 1964), which at small n provide good accuracy and yield the easy inversion of Laplace transformation—either with the help of the above integral equations, or through expansion of polynomials into common fractions and use of residue theory.

References

Abramowitz, M., Stegun, I., 1964. Handbook of Mathematical Functions. U.S. National Bureau of Standards. Applied Mathematics Series 55.

Bateman, G., Erdelyi, A., 1953. Higher transcendental functions: Bessel functions, functions of parabolic cylinder, orthogonal polynomials. McGraw-Hill, New York.

Bateman, G., Erdelyi, A., 1954. Tables of integral transforms: In 2 volumes. McGraw-Hill, New York.

Kubenko, V.D., 1979. Non-stationary interaction of structural elements with the medium. Naukova dumka, Kyiv (in Russian).

Kubenko, V.D., 2006. Impact of a long thin body on a cylindrical cavity in liquid: a plain problem. International Applied Mechanics 6, 1185–1225.

Logvinovich, G.V., 1969. Hydrodynamics of currents with free boundaries. Naukova dumka, Kyiv (in Russian).

Morse, F.M., Feshbach, H., 1953. Methods of Theoretical Physics: In 2 Volumes. McGraw-Hill, New York.

Paryshev, E.V., 2003. Mathematical modeling of unsteady cavity flows. Fifth International Symposium on Cavitation (CAV 2003). Osaka, Japan, 1–18.

Savchenko, Y.N., 1998. High-speed body motion at supercavitating flow. Proceedings of the Third International Symposium on Cavitation. Grenoble, France, pp. 9–14.

Savchenko, Yu.N., Vlasenko, Yu.D., Semenenko, V.N., 1999. Experimental study of high-speed cavitated flows. International Journal of Fluid Mechanics Research 3, 365–374.

Young, Y.L., 2007. Time-dependent hydroelastic analysis of cavitating propulsors. Journal of Fluids and Structures 23, 269–295.